ISSN 2075-8545 (online)

Nanotechnologies in construction
Нанотехнологии в строительстве

2026; 18 (2):
210–231

Nanobuild.ru

APPLICATION OF NANOMATERIALS AND NANOTECHNOLOGIES IN CONSTRUCTION



Original article
https://doi.org/10.15828/2075-8545-2026-18-2-210-231

# Synthesis of an active substance for microcapsules in a polymer composite with a self-healing effect

**Natalia I. Cherkashina[1], Vyacheslav I. Pavlenko[1], Sergey V. Serebryakov[1], Artem Yu. Ruchiy[1]*, Yulia M. Samoylova[2]**

[1] Belgorod State Technological University named after V.G. Shukhov, 308012, Belgorod, Kostyukova str., 46, Russian Federation

[2] Belgorod Law Institute of the Ministry of Internal Affairs of the Russian Federation named after I.D. Putilin, 71 Gorky St., Belgorod, 308024, Russian Federation

* Corresponding author: e-mail: artiem.ruchii.99@mail.ru

**ABSTRACT**

**Introduction.** The aim of this study is to examine the properties of a synthesized epoxy resin hardener based on dicyclopentadiene and maleic anhydride. **Materials and methods.** The following chemical reagents were used for synthesis: dicyclopentadiene 98%, maleic anhydride (technical), trichloromethane (C.P.). The research was carried out with the Sintecor IR 10 FTIR spectrometer, the STA 449 F1 Jupiter thermogravimetric analyzer. **Results and discussion.** Studying the initial substances allowed the calculated and experimental data to be correlated. Subsequent operations then revealed the structure and thermal properties of the obtained adduct. **Conclusion.** As a result of this research, an epoxy resin hardener has been obtained that can withstand a wide range of temperature variations. The synthesized substance is expected to find practical application in self-healing polymer composites.

**KEYWORDS:** dicyclopentadiene, maleic anhydride, Diels-Alder reaction, polymer composite, FT-IR spectroscopy, thermogravimetry, functional density theory

**ACKNOWLEDGEMENTS:** The study was supported by a grant from the Russian Science Foundation No 24-79-10033 https://rscf.ru/project/24-79-10033/ using equipment on the basis of the Center for High Technologies of BSTU named after V. G. Shukhov.

**FOR CITATION:**
Cherkashina N.I., Pavlenko V.I., Serebryakov S.V., Ruchiy A.Yu., Samoylova Yu.M. Synthesis of an active substance for microcapsules in a polymer composite with a self-healing effect. *Nanotechnologies in Construction.* 2026; 18(2):210–231. https://doi.org/10.15828/2075-8545-2026-18-2-210-231. – EDN: XWXZHG.

# Синтез активного вещества для микрокапсул в полимерном композите с эффектом самозалечивания

**Наталья Игоревна Черкашина[1], Вячеслав Иванович Павленко[1], Сергей Викторович Серебряков[1], Артём Юрьевич Ручий[1]*, Юлия Михайловна Самойлова[2]**

[1] Белгородский государственный технологический университет им. В.Г. Шухова, 308012, г. Белгород, ул. Костюкова 46, Российская Федерация

[2] Белгородский юридический институт Министерства внутренних дел Российской Федерации имени И.Д. Путилина, 308024, г. Белгород, ул. Горького 71, Российская Федерация

* Автор, ответственный за переписку: e-mail: artiem.ruchii.99@mail.ru

**АННОТАЦИЯ**

**Введение.** Исследование направлено на изучение свойств синтезированного отвердителя для эпоксидной смолы на основе дициклопентадиена и малеинового ангидрида. **Материалы и методы исследования.** Для осуществления синтеза приме-

ISSN 2075-8545 (online)

Nanotechnologies in construction
Нанотехнологии в строительстве

2026; 18 (2):
210–231

Nanobuild.ru

APPLICATION OF NANOMATERIALS AND NANOTECHNOLOGIES IN CONSTRUCTION

нялись следующие химические реактивы: дициклопентадиен 98%, малеиновый ангидрид (технический), трихлорметан (ХЧ). Исследования проводились с помощью ИК-Фурье спектрометра Sintecor IR 10, термогравиметрического анализатора STA 449 F1 Jupiter. Расчеты велись с помощью пакета программ QChem и IQmol. **Результаты и обсуждение.** Исследование исходных веществ позволило соотнести расчетные и экспериментальные данные. Последующие операции позволили определить структуру полученного аддукта и его термические характеристики. **Заключение.** В результате работы получен отвердитель для эпоксидных смол, выдерживающий широкий спектр температурного воздействия. Синтезированное вещество найдет практическое применение в самозалечивающихся полимерных композитах.

**КЛЮЧЕВЫЕ СЛОВА:** дициклопентадиен, малеиновый ангидрид, реакция Дильса-Альдера, полимерный композит, ИК-Фурье спектроскопия, термогравиметрия, теория функциональной плотности

**БЛАГОДАРНОСТИ:** Исследование выполнено за счет гранта Российского научного фонда № 24-79-10033 https://rscf.ru/project/24-79-10033/ с использованием оборудования на базе Центра высоких технологий БГТУ им. В. Г. Шухова.

**ДЛЯ ЦИТИРОВАНИЯ:**
Черкашина Н.И., Павленко В.И., Серебряков С.В., Ручий А.Ю., Самойлова Ю.М. Синтез активного вещества для микрокапсул в полимерном композите с эффектом самозалечивания. *Нанотехнологии в строительстве.* 2026;18(2):210–231. https://doi.org/10.15828/2075-8545-2026-18-2-210-231. – EDN: XWXZHG.

## INTRODUCTION

Modern autonomous self-healing systems represent a key approach to improving the durability of polymer composites, which are widely used in construction, aviation, energy, medicine, and the space industry. Under operating conditions, minor mechanical damage occurs, leading to a decrease in the material's performance properties and durability [1–4]. Microencapsulated active substances released locally upon damage initiate polymerization reactions, restoring the integrity of structures and part of the strength characteristics [5–10].

Self-healing (self-restoration) of synthetic material is a partial or complete reduction of the damage area due to mass transfer and consolidation of crack boundaries, which leads to partial or complete restoration of the functional properties of the material. In such systems, damage consolidation (self-healing) occurs after crack consolidation provided by mass transfer [11, 12]. Processes can occur autonomously (for example, through the flow of matter within the material) or non-autonomously, where healing is triggered by external stimuli such as elevated temperature or ultraviolet radiation. [13, 14]. Self-healing mechanisms are divided into external and internal types according to their organization. External mechanisms depend on embedded healing agents (e.g., microcapsules with healing substances), while internal mechanisms need no additional repair compounds [15–22].

This research aims at the synthesis of an active substance based on the Diels-Alder reaction between dicyclopentadiene (DCPD) and maleic anhydride (MA). As a result of the reaction, cracks in the polymer composite heal. This interaction is a classic (4+2)-cycloaddition, in which maleic anhydride acts as a highly effective dienophile. Due to its two electron-acceptor carbonyl groups, which reduce the energy of HCMO (LUMO) (lowest unoccupied molecular orbital), it is able to react with a wide range of conjugated dienes to form the corresponding anhydrides.

In particular, maleic anhydride readily reacts with both acyclic dienes (butadiene, isoprene) and cyclic structures, including cyclopentadiene and polycyclic aromatic compounds such as anthracene [23, 24]. It is this high reactivity that makes it an ideal candidate for the design of molecular building blocks needed to create advanced functional materials with self-healing properties.

The need for such syntheses is dictated by the practical challenges of materials science. When external factors (temperature, humidity) make it difficult to produce stable two-component epoxy plastics, pre-synthesized stable hardeners are required.

## MATERIALS, EQUIPMENT, RESEARCH METHODS

### Materials

The following reagents were used in the course of the research: dicyclopentadiene ($C_{10}H_{12}$) 98% produced by ACMEC biomechanical Co.ltd Shanghai; trichloromethane ($CHCl_3$) C.P. produced by «ECOS-1» JSC, Moscow; maleic anhydride ($C_4H_2O_3$) technical.

### Equipment and research methods

DFT calculations were carried out using the QChem 6.4 program and interpreted in the IQmol 3.1.5 program.

Imaging of FT-IR spectra of compounds was carried out with Sintecor IR 10 in the wavenumber range of 470–4000 $cm^{-1}$.

Thermogravimetric analysis of the compounds was performed on the STA 449 F1 Jupiter instrument. The samples were heated from 20 to 400 °C at a rate of 10 deg/min in the following atmosphere: 21% $O_2$, 79% Ar.

ISSN 2075-8545 (online)



## RESULTS AND DISCUSSION

### 1. Experimental part

In [25], which focuses on developing capsules containing a healing agent for composites, insufficient attention was paid to the compound that acts as the active species for initiating the chemical reaction.

Dicyclopentadiene (Fig. 1a) is a high-tension molecule with a norbornene base and an adjacent cyclopentene ring. Under normal conditions, it is a viscous liquid with a pungent odor. In general, organic anhydrides and amines are used as hardeners for two-component epoxy systems. In our research we have chosen the anhydride terminus of the molecule as the reaction radical. Maleic anhydride was used as a precursor (Fig. 1b).

In the reaction, it is important to observe the temperature regime (not exceeding 80 °C), since at high temperatures dicyclopentadiene breaks down into 2 molecules of cyclopentadiene. However, the Diels-Alder reaction does not require high temperatures.

In the early studies, high temperatures (160–200 °C) were mostly used for the Diels-Alder reaction using dicyclopentadiene [21].

The Diels-Alder reaction is based on the ability of dienophiles to attach to dienes with low molecular orbital density. Molecular densities were calculated using the QChem program. The calculations were carried out using the Hartree-Fock (HF) method, which is an approximate solution of the Schrödinger equation. Fig. 2 shows a model of molecular orbitals of maleic anhydride.

The parameters of the molecule are specified in the FChk format. The spatial coordinates of the molecule are presented in the Table 1.

The basis for quantum chemical calculations is 6-31G, as this basis is excellent for the calculations of medium-complex systems that do not contain heavy atoms.

The Hartree–Fock model does not provide the most accurate description of molecular structure and its behavior, as it reduces the system to the outer shells of the constituent atoms while neglecting the contribution of inner electrons. Nevertheless, a quantum system obtained via the HF method can be correlated with experimental data.

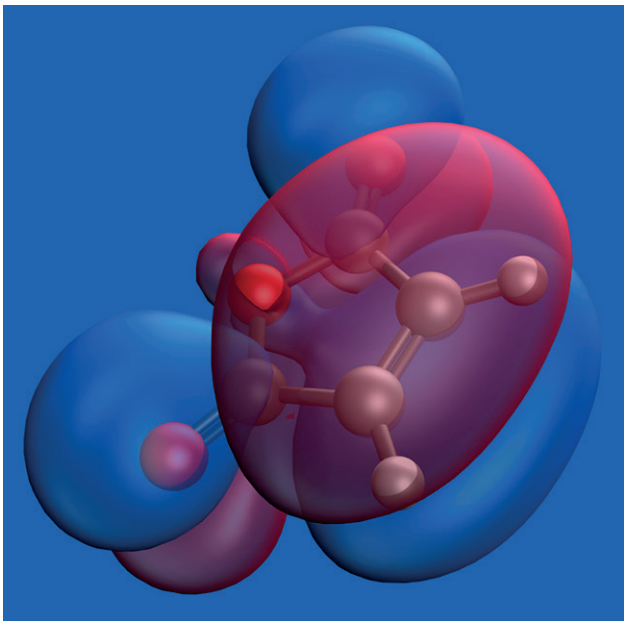

**Fig. 2.** Model of a maleic anhydride molecule with isolated molecular orbitals

Molecular orbitals of dicyclopentadiene were also modeled. The result is presented in Fig. 3.

The spatial coordinates of the dicyclopentadiene molecule are presented in the Table 2.

The reaction between dicyclopentadiene and maleic anhydride was carried out in dried chloroform in a nitrogen medium. As the Diels-Alder mechanism (Fig. 4) provides, the reaction takes place without transition states with the breaking of double bonds at low activation energy.

The peculiarity of the Diels-Alder reaction is that it takes place mainly with aromatic cycles. The calculated

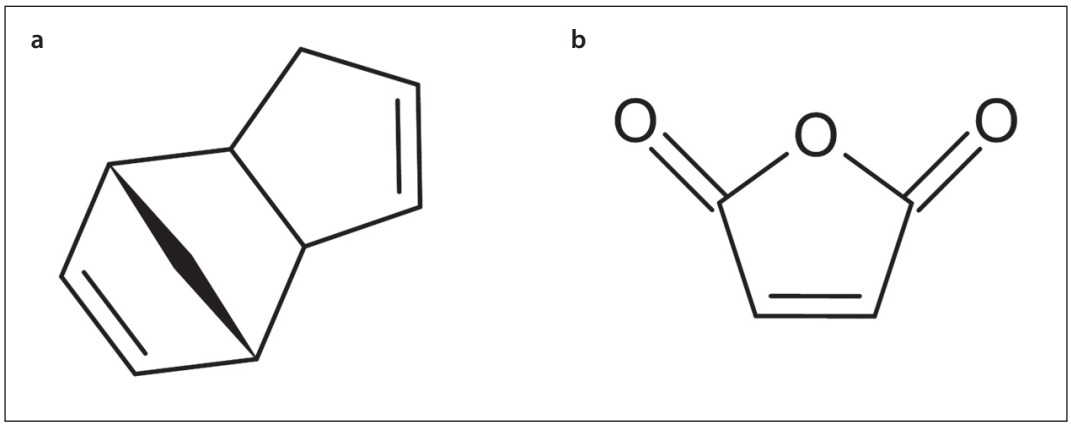


**Fig. 1.** Structural formula: a) DCPD; b) MA

ISSN 2075-8545 (online)



**Table 1.** Spatial coordinates of the MA molecule

| 01* | | | |
|---|---|---|---|
| **Atom** | **x** | **y** | **z** |
| C | 0.6623095 | –1.2489674 | 0.0000000 |
| C | –0.6623106 | –1.2489670 | 0.0000000 |
| C | –1.1376593 | 0.1599721 | 0.0000000 |
| C | 1.1376590 | 0.1599714 | 0.0000000 |
| O | 0.0000001 | 0.9570981 | 0.0000000 |
| O | 2.2470393 | 0.5977750 | 0.0000000 |
| O | –2.2470392 | 0.5977764 | 0.0000000 |
| H | 1.3356524 | –2.0762104 | 0.0000000 |
| H | –1.3356540 | –2.0762096 | 0.0000000 |

* Indication of the number of objects in the coordinate area (0 – free space, 1 – molecule)

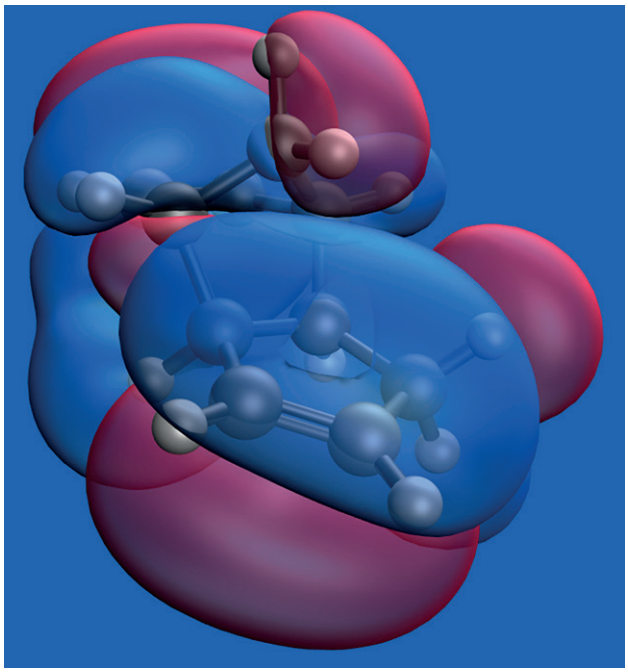

**Fig. 3.** A model of a dicyclopentadiene molecule with isolated molecular orbitals.

NMR spectrum of dicyclopentadiene (Fig. 5) indicates the aromaticity of this compound. The results of the calculation are presented in the Table 3.

The results of the calculation indicate a spectrum shift in the region of ~8 and ~7 ppm, which meets the aromaticity conditions of the compound.

The reaction was monitored using FT-IR spectroscopy. The analysis was performed with a Sintecor IR10 spectrometer in potassium bromide tablets.

In the FT-IR spectra of maleic anhydride (Fig. 6, Table 4), the modes characteristic of aromatic heterocycles (~1240 and ~ 1059 cm-1) is traced, and it is also worth emphasizing that the obtained spectra are identical to those specified in the literature [26].

In the FT-IR spectra of dicyclopentadiene (Fig. 7, Table 5), vibrational modes characteristic of cyclic compounds with the presence of double bonds are traced.

The FT-IR spectrum of the dicyclopentadiene and maleic anhydride adduct (Fig. 8, Table 6) has few modes in common with the initial compounds. This is due to the complex three-dimensional geometry of the adduct in conjunction with the variety of conformations of the compound.

Figure 9 clearly shows the discrepancy between the vibrational modes of the adduct and the initial compounds (DCPD and MA), which directly indicates the formation of a new compound.

## 2. Calculation part

To confirm the results of the synthesis, calculations were made of the frequencies of oscillations of molecular bonds. It is known that each frequency of bond oscillation has its own shear tensor, which depends on the density of bonds and shifts the frequency of radiation. The shear tensor was selected on the basis of the selection of real and calculated FTIR data of the spectra of the initial substances. The resulting scale factor was 0.905 for both dicyclopentadiene (Fig. 10, Table 7) and maleic anhydride (Fig. 11, Table 8) and was set for the most intense modes.

Fig. 11. Visual correlation of experimental (top) and calculated (bottom) oscillatory modes of MA

Referring to the design of the experiment, the formula of the resulting compound should contain two combined norbornenoric rings with an anhydride appendage (Fig. 12).

However, the obtained FT-IR spectroscopy data (Fig. 13) do not fully coincide with the calculated data (Tables 9–12), which indicates that a mixture of substances

ISSN 2075-8545 (online)



**Table 2.** Spatial coordinates of the DCPD molecule

| 01 | | | |
|---|---|---|---|
| **Atom** | **x** | **y** | **z** |
| C | 2.4796350 | 0.1410729 | –0.0683041 |
| C | 1.6804108 | 1.1941252 | 0.1057580 |
| C | 1.7488112 | –1.1630978 | 0.0926355 |
| C | 0.3643315 | –0.7244309 | 0.4318390 |
| C | 0.3472054 | 0.7291123 | 0.4609470 |
| C | –0.8958314 | 1.0722448 | –0.2545958 |
| C | –0.8628465 | –1.0467290 | –0.3273888 |
| C | –2.0541842 | –0.7067548 | 0.4813796 |
| C | –2.0739739 | 0.6378653 | 0.5295530 |
| C | –0.8910027 | 0.0509215 | –1.3260295 |
| H | 3.4853189 | 0.2129811 | –0.2884243 |
| H | 1.9620733 | 2.1817942 | 0.0047628 |
| H | 2.1725093 | –1.7477525 | 0.8822929 |
| H | 1.7956651 | –1.7857229 | –0.7762965 |
| H | 0.2584193 | –1.3209837 | 1.3137729 |
| H | 0.2439873 | 1.2754131 | 1.3751688 |
| H | –0.9388543 | 2.1120129 | –0.5034561 |
| H | –0.8677873 | –2.0639699 | –0.6591968 |
| H | –2.7252416 | –1.3599432 | 0.9150281 |
| H | –2.7627270 | 1.2376484 | 1.0100771 |
| H | –0.0244552 | 0.0867506 | –1.9526967 |
| H | –1.6542394 | 0.0657942 | –2.0757952 |

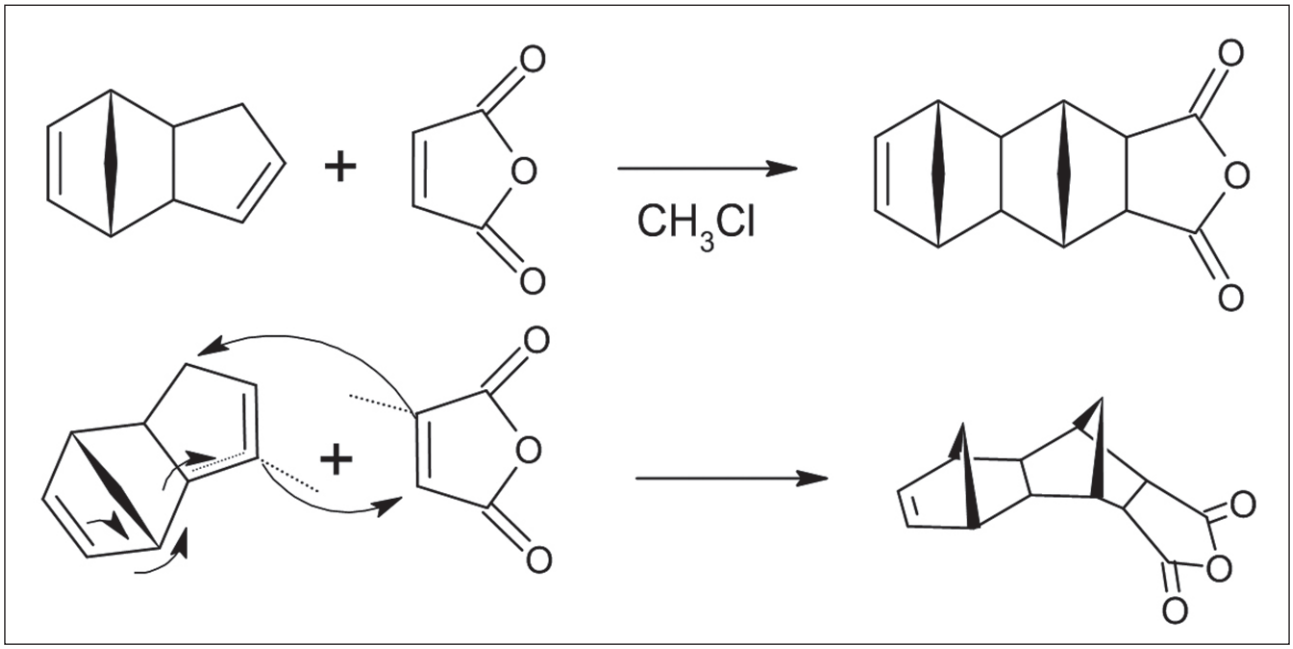


**Fig. 4.** Mechanism of the Diels-Alder reaction for DCPD and MA

ISSN 2075-8545 (online)



**Table 3.** Magnetic Resonance Values of Hydrogen Atoms in DCPD

| Atom | Chemical shift, m.d. | | | | | | | | | | | |
|---|---|---|---|---|---|---|---|---|---|---|---|---|
| 1H | 6.93 | 7.01 | 3.30 | 2.82 | 2.99 | 3.40 | 2.96 | 2.87 | 8.06 | 8.00 | 2.90 | 2.41 |

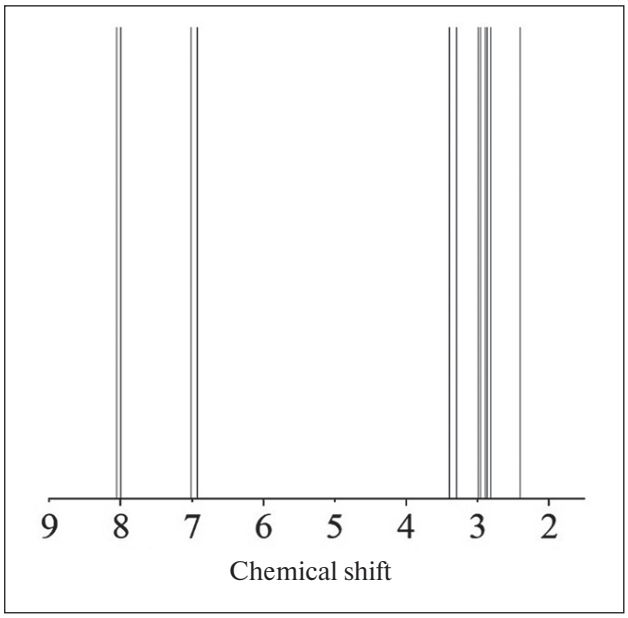


**Fig. 5.** Calculated NMR spectrum of DCPD

has been obtained. Namely, the presence of a fraction of anhydride hydrolyzed to carboxylic acid in the mixture, together with the incomplete convergence, was affected by the various conformations of the compounds.

The acid-type adduct molecule (Fig. 11) is a nonlinear molecule, which means that the number of permissible modes satisfies the formula 3N-6 (where N is the number of atoms in the molecule).

According to the models presented in Fig. 14 and 15 trace the complex spatial structure of acid-type and anhydride adduct molecules, which in the future will increase

**Table 4.** Interpretation of MA oscillatory modes

| Absorption area, $cm^{-1}$ | Characteristics |
|---|---|
| 1853 | v C=O (in cyclic anhydrides) |
| 1782 | v C=O (in cyclic anhydrides) |
| 1632 | C=C (conjugate with C=O) |
| 1240 | aromatic and vinyl (=C–O–C–) |
| 1059 | aromatic and vinyl (=C–O–C–) |

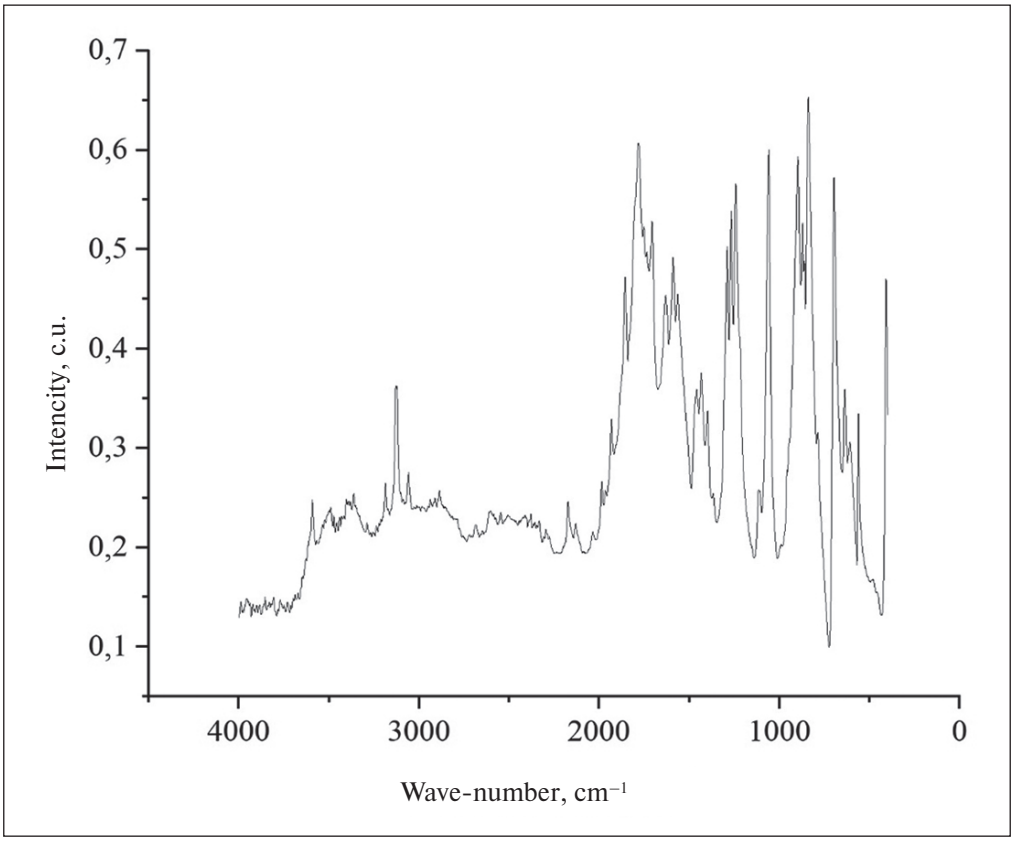


**Fig. 6.** FT-IR spectrum of maleic anhydride

ISSN 2075-8545 (online)



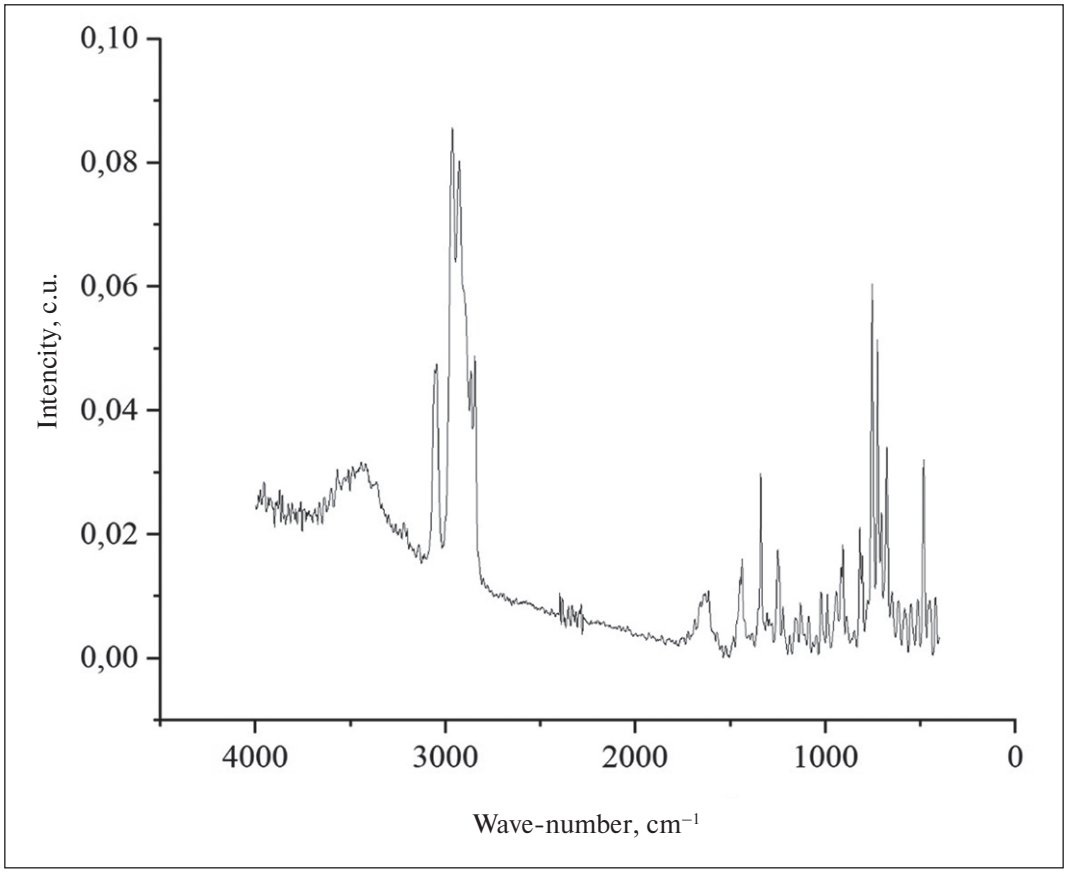


**Fig. 7.** FT-IR spectrum of dicyclopentadiene

**Table 5.** Deciphering the oscillatory modes of DCPD

| Absorption area, $cm^{-1}$ | Characteristics |
|---|---|
| 3048 | v as HRC=$CH^2$ |
| 2962 | –$CH^2$– |
| 2924 | –$CH^2$– |
| 2844 | –$CH^2$– |
| 1439 | –$CH^2$– |
| 1336 | =CH |
| 1250 | δ (ar C–H)ip (in-plane vibrations) |
| 912 | δ C=C |
| 815, 750, 728, 680 | 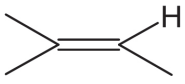 |

ISSN 2075-8545 (online)



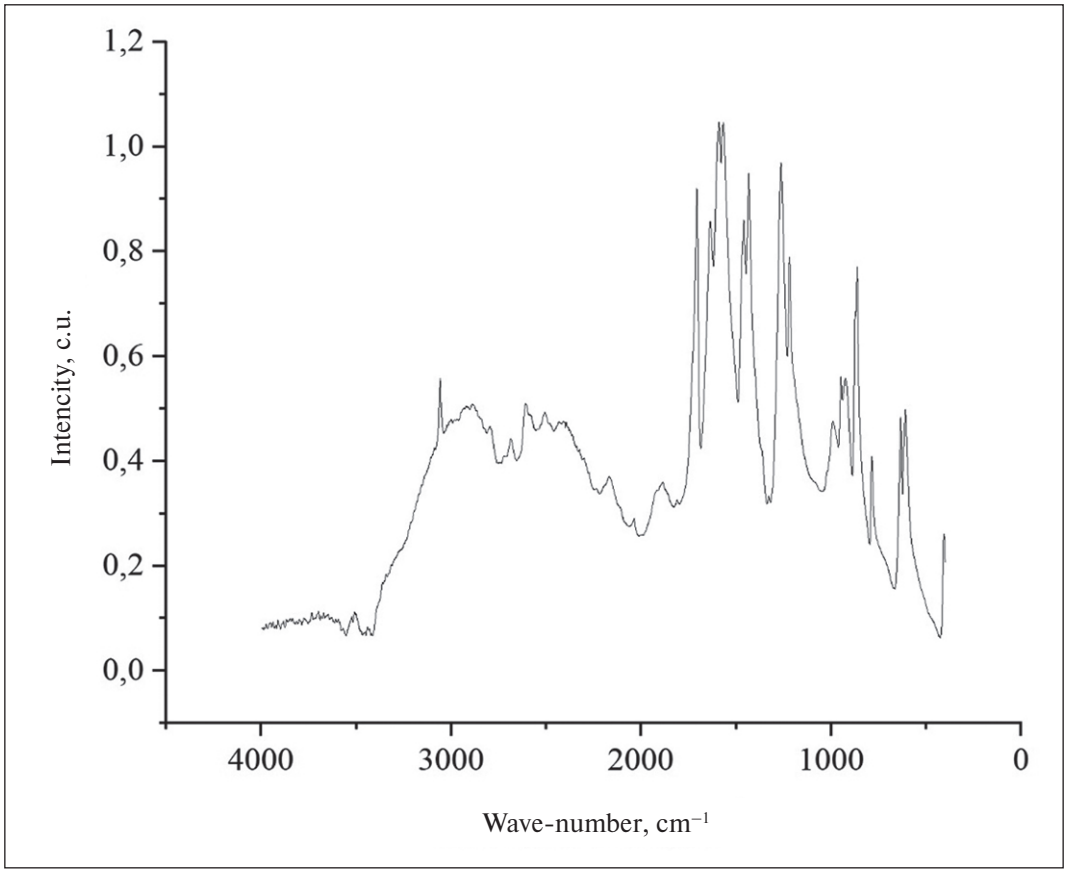


**Fig. 8.** FT-IR spectrum of DCPD and MA adduct

**Table 6.** Interpretation of the vibrational modes of the DCPD and MA adduct

| Absorption area, $cm^{-1}$ | Characteristics |
|---|---|
| 3062 | v as $HRC=CH_2$ |
| 1708 | Aromatic aldehydes |
| 1585 | v ar |
| 1429 | $CH_2$–C=O |
| 1265 | Aromatic Acid Ester |
| 1215 | v C–O st |

ISSN 2075-8545 (online)



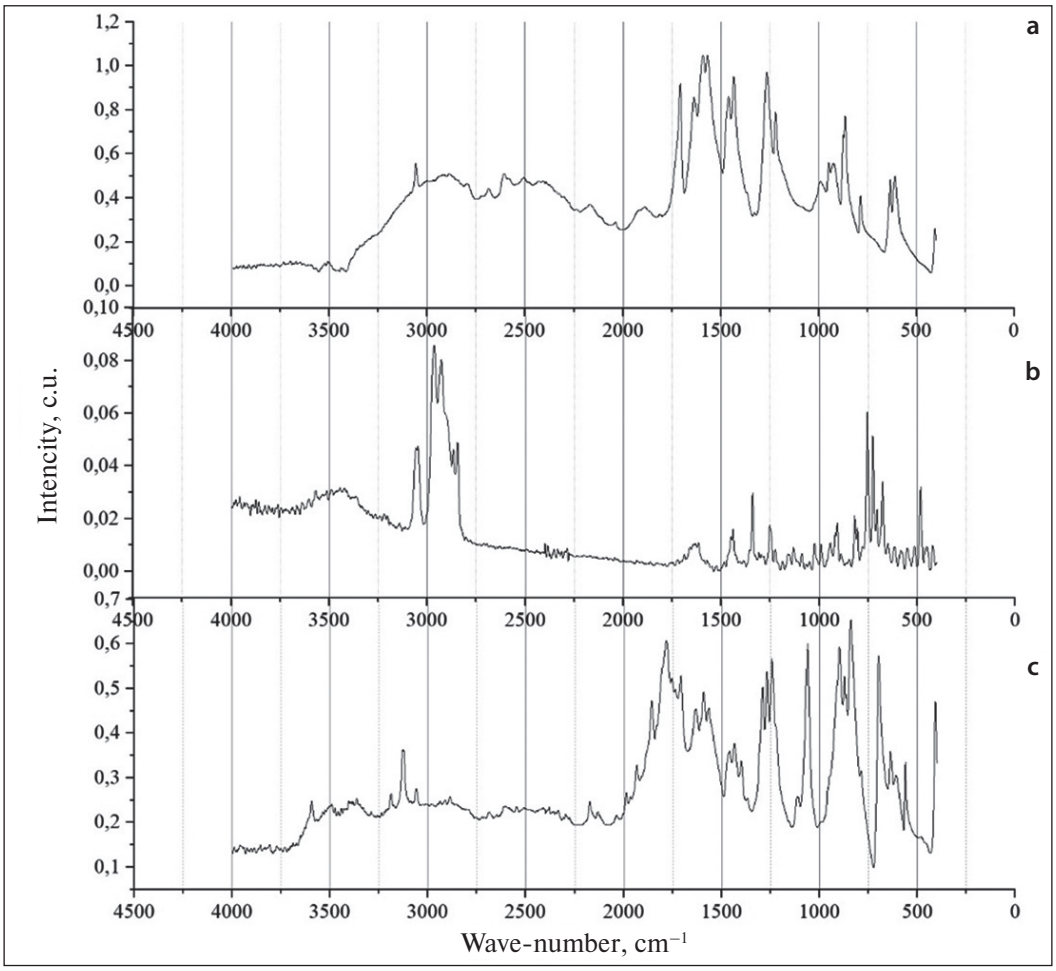


**Fig. 9.** Comparison of FT-IR spectra: a) adduct; b) DCPD; c) MA

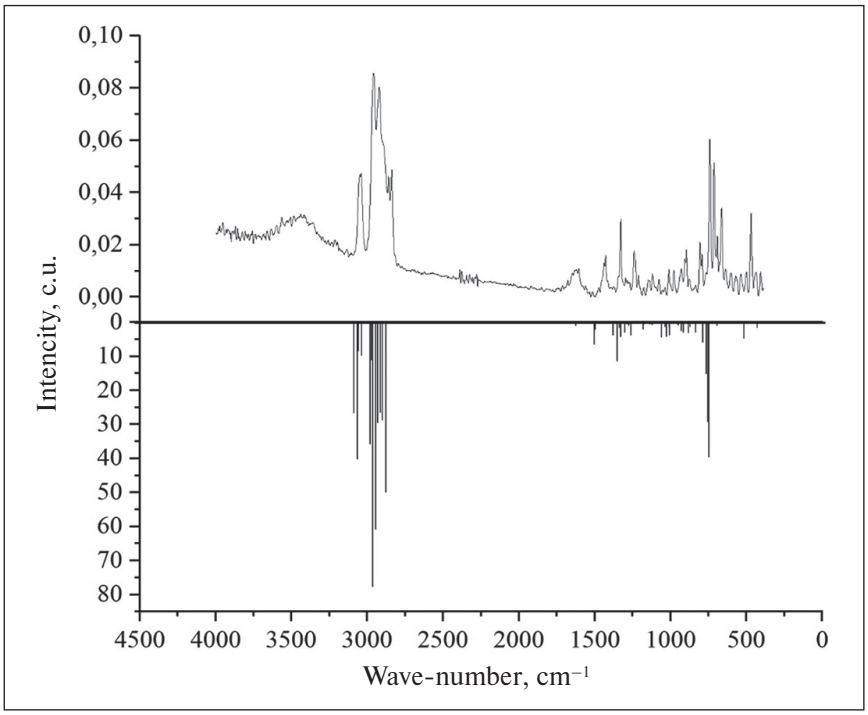


**Fig. 10.** Visual correlation of experimental (top) and calculated (bottom) oscillatory modes of DCPD

ISSN 2075-8545 (online)



**Table 7.** Estimated FT-IR spectroscopy values for CPDD

| Frequency, $cm^{-1}$ | Intensity, km/mol | Frequency, GHz |
|---|---|---|
| 428.05 | 1.538 | 12832.61616 |
| 443.84 | 0.256 | 13305.98846 |
| 514.62 | 4.706 | 15427.91947 |
| 634.13 | 0.337 | 19010.73914 |
| 691.25 | 0.952 | 20723.15366 |
| 745.55 | 39.513 | 22351.02671 |
| 754.86 | 29.19 | 22630.13348 |
| 763.49 | 15.155 | 22888.85438 |
| 788.49 | 5.915 | 23638.33552 |
| 834.86 | 2.925 | 25028.47315 |
| 871.33 | 1.31 | 26121.81624 |
| 881.14 | 3.061 | 26415.91264 |
| 892.25 | 0.095 | 26748.98207 |
| 915.66 | 2.874 | 27450.79621 |
| 929.45 | 2.451 | 27864.21001 |
| 949.67 | 0.896 | 28470.39036 |
| 975.62 | 0.096 | 29248.35179 |
| 1004.6 | 3.812 | 30117.15033 |
| 1008.56 | 1.351 | 30235.86814 |
| 1023.96 | 4.053 | 30697.54853 |
| 1034.88 | 1.31 | 31024.92189 |
| 1037.16 | 1.296 | 31093.27457 |
| 1058.63 | 4.365 | 31736.92898 |
| 1118.38 | 0.705 | 33528.18892 |
| 1125.83 | 0.311 | 33751.5343 |
| 1138 | 0.547 | 34116.38172 |
| 1173.75 | 0.63 | 35188.13976 |
| 1180.26 | 2.096 | 35383.30465 |
| 1207.66 | 0.27 | 36204.73598 |
| 1261.29 | 3.746 | 37812.52294 |
| 1274.11 | 1.019 | 38196.85687 |
| 1282.7 | 0.536 | 38454.37859 |
| 1299.4 | 2.922 | 38955.03199 |
| 1304.4 | 0.133 | 39104.92822 |
| 1327.05 | 4.215 | 39783.95814 |
| 1337.37 | 1.656 | 40093.34396 |
| 1339.31 | 0.27 | 40151.50369 |
| 1350.23 | 11.368 | 40478.87706 |
| 1377.01 | 3.887 | 41281.72126 |
| 1495.96 | 2.045 | 44847.75255 |
| 1502.75 | 6.502 | 45051.31163 |
| 1623.81 | 0.939 | 48680.59912 |
| 1667.57 | 0.3 | 49992.49092 |
| 2876.06 | 49.931 | 86222.10968 |
| 2900.43 | 28.764 | 86952.7039 |
| 2911.82 | 26.492 | 87294.16751 |
| 2930.43 | 29.431 | 87852.08127 |
| 2944.63 | 60.856 | 88277.78656 |
| 2963.09 | 77.664 | 88831.20344 |
| 2970.26 | 11.14 | 89046.15463 |
| 2979.99 | 35.781 | 89337.85269 |
| 3037.22 | 9.784 | 91053.56493 |
| 3058.85 | 8.456 | 91702.01602 |
| 3065.99 | 40.144 | 91916.06783 |
| 3087.53 | 26.654 | 92561.82078 |

ISSN 2075-8545 (online)



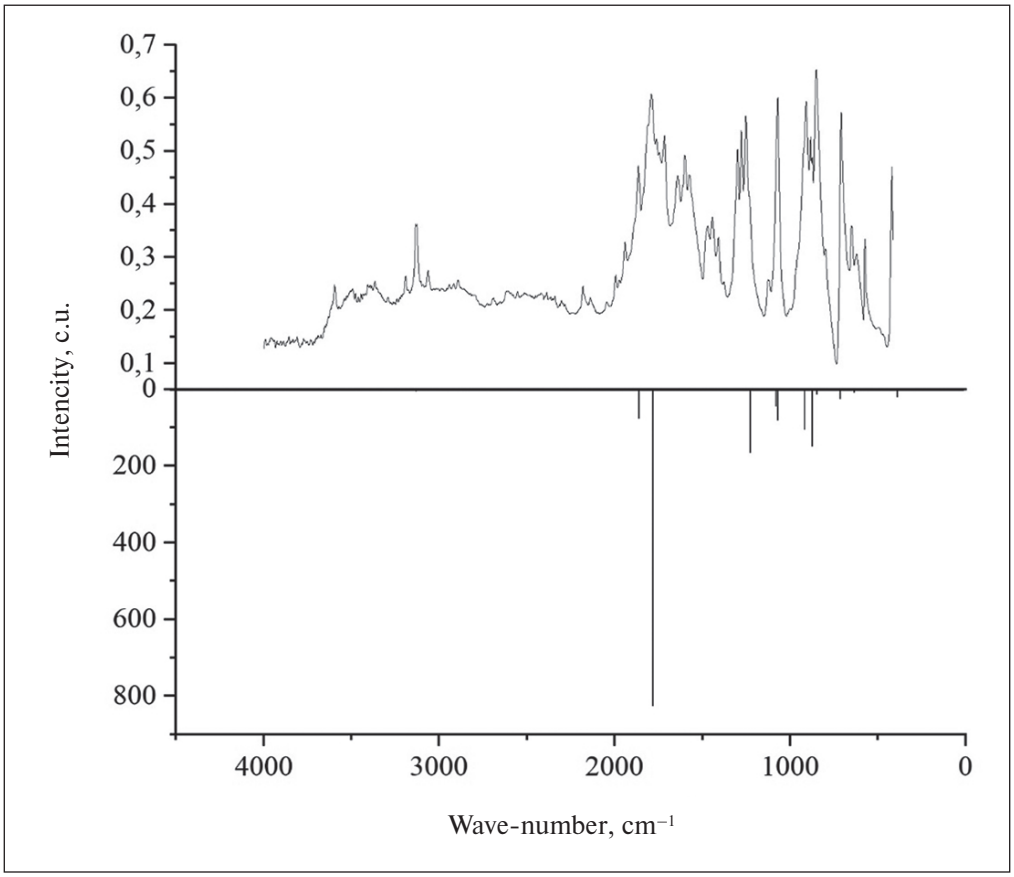


**Fig. 11.** Visual correlation of experimental (top) and calculated (bottom) oscillatory modes of MA

**Table 8.** Calculated FT-IR spectroscopy values for MA

| Frequency, $cm^{-1}$ | Intensity, km/mol | Frequency, GHz |
|---|---|---|
| 389.58 | 20.435 | 11679.31458 |
| 541.85 | 2.723 | 16244.25434 |
| 624.48 | 1.143 | 18721.43942 |
| 634.17 | 8.008 | 19011.93831 |
| 715.12 | 25.234 | 21438.75826 |
| 848.37 | 12.421 | 25433.49276 |
| 873.53 | 148.693 | 26187.77058 |
| 916.46 | 104.567 | 27474.77961 |
| 1069.96 | 80.398 | 32076.59384 |
| 1078.17 | 43.965 | 32322.72344 |
| 1225.12 | 165.313 | 36728.17361 |
| 1336.65 | 1.2 | 40071.7589 |
| 1634.12 | 0.78 | 48989.68515 |
| 1781.76 | 824.756 | 53415.821 |
| 1860.36 | 75.998 | 55772.18972 |
| 3132.14 | 5.095 | 93899.19494 |
| 3153.54 | 2.576 | 94540.7508 |

ISSN 2075-8545 (online)
Nanotechnologies in construction
Нанотехнологии в строительстве
2026; 18 (2):
210–231



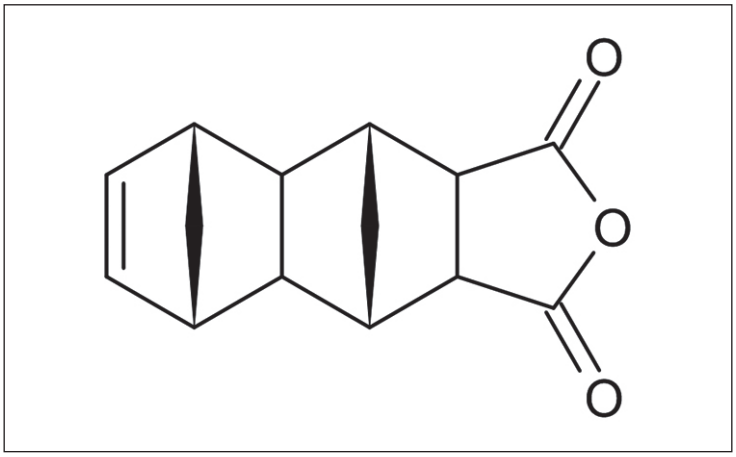


**Fig. 12.** Structural Formula of Adduct

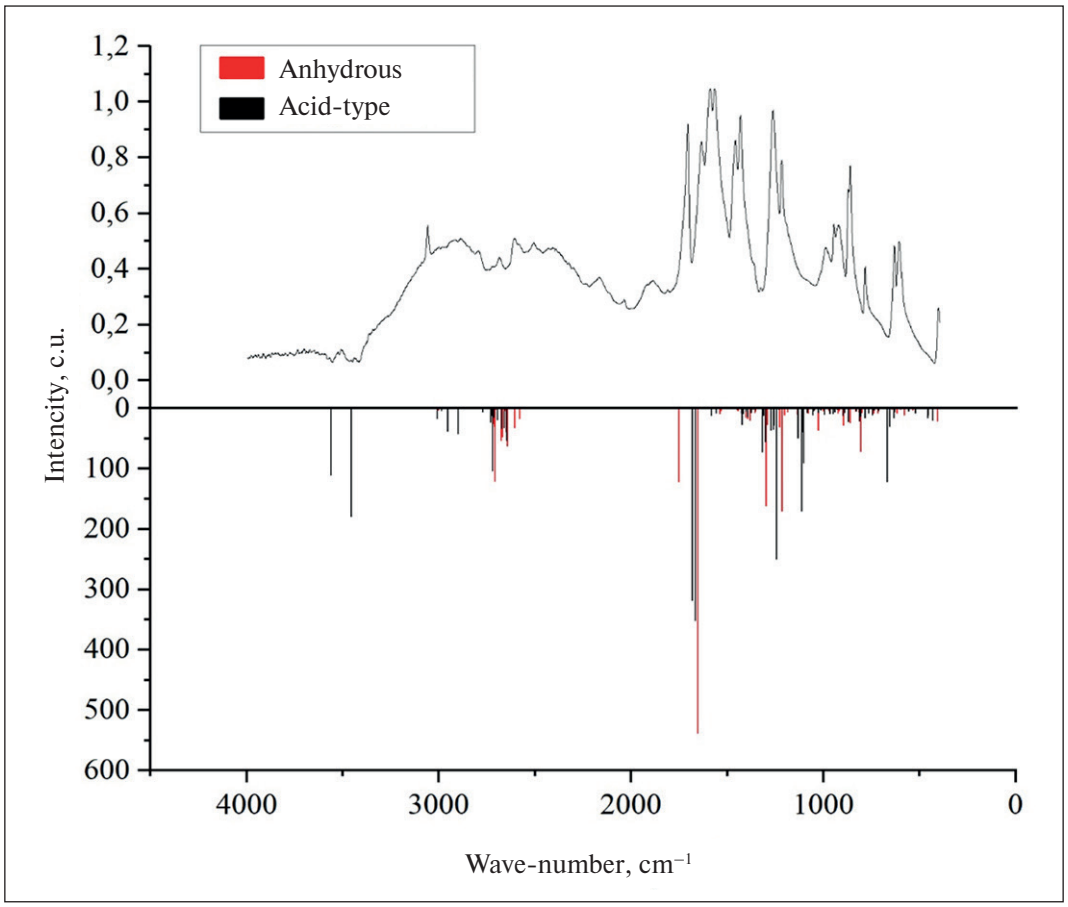


**Fig. 13.** Visual Ratio of Experimental (Top) and Calculated (Bottom) Oscillatory Modes of Adduct

ISSN 2075-8545 (online)



**Table 9.** Spatial coordinates of acid-type adduct

| 01 | | | |
|---|---|---|---|
| **Atom** | **x** | **y** | **z** |
| C | 2.9315102 | –0.4174406 | 1.6091419 |
| C | 3.0254627 | 0.9295588 | 1.3136708 |
| C | 2.5569832 | 1.0810698 | –0.1118783 |
| C | 2.4354607 | –1.0829987 | 0.3549941 |
| C | 1.0075778 | 0.8395233 | –0.0474390 |
| C | 0.9366974 | –0.6749013 | 0.1934086 |
| C | 3.1804623 | –0.2181038 | –0.6485449 |
| C | 0.0885279 | 1.0442277 | –1.2931481 |
| C | 0.1326389 | –1.1619874 | –1.0557912 |
| C | 0.4111278 | –0.1415290 | –2.1722666 |
| C | –1.3729620 | –0.8532875 | –0.8165288 |
| C | –1.3983933 | 0.7122421 | –0.9406452 |
| C | –1.9957753 | –1.6446249 | 0.3355181 |
| C | –2.0030276 | 1.5651346 | 0.1580316 |
| O | –1.7881948 | –2.8468094 | 0.3722530 |
| O | –2.9465504 | 2.2957288 | –0.1068009 |
| H | 3.2705296 | –0.8883887 | 2.5219852 |
| H | 3.4448724 | 1.6890988 | 1.9595683 |
| H | 2.8475685 | 2.0572784 | –0.5530969 |
| H | 2.6120350 | –2.1790877 | 0.3454574 |
| H | 0.6533427 | 1.4831682 | 0.7777780 |
| H | 0.4022466 | –0.9818845 | 1.1194377 |
| H | 4.2915592 | –0.2513373 | –0.5230865 |
| H | 3.0402717 | –0.5105674 | –1.6868551 |
| H | 0.1937191 | 2.0531199 | –1.7463991 |
| H | 0.2912302 | –2.2359798 | –1.2932265 |
| H | 1.3958228 | –0.0862649 | –2.6267948 |
| H | –0.2666615 | –0.2484397 | –3.0524763 |
| H | –1.8902733 | –1.2555622 | –1.7204702 |
| H | –1.9918819 | 0.9341792 | –1.8604735 |
| O | –1.5394470 | 1.5213264 | 1.4257724 |
| O | –2.8230620 | –1.1274285 | 1.2703571 |
| H | –1.9304899 | 2.0635870 | 2.1254570 |
| H | –3.2036012 | –0.2467562 | 1.2494032 |

ISSN 2075-8545 (online)



**Table 10.** Calculated FT-IR spectroscopy values for acid-type adduct

| Frequency, $cm^{-1}$ | Intensity, km/mol | Frequency, GHz |
|---|---|---|
| 422.57 | 20.269 | 12668.3299 |
| 447.17 | 11.099 | 13405.81934 |
| 450.67 | 16.077 | 13510.7467 |
| 512.86 | 7.682 | 15375.156 |
| 549.09 | 5.115 | 16461.30408 |
| 623.69 | 4.113 | 18697.75581 |
| 624.58 | 15.528 | 18724.43734 |
| 648.84 | 29.641 | 19451.73384 |
| 659.62 | 121.386 | 19774.91011 |
| 705.31 | 3.605 | 21144.66186 |
| 728.38 | 2.813 | 21836.28306 |
| 736.44 | 11.004 | 22077.91578 |
| 758.08 | 8.117 | 22726.66666 |
| 776.43 | 16.301 | 23276.78582 |
| 797.25 | 12.662 | 23900.95371 |
| 803.67 | 20.553 | 24093.42047 |
| 820.49 | 4.897 | 24597.67139 |
| 839.18 | 1.083 | 25157.98349 |
| 860.86 | 22.029 | 25807.93354 |
| 881.8 | 6.678 | 26435.69895 |
| 891.52 | 12.292 | 26727.09722 |
| 918.94 | 2.097 | 27549.12814 |
| 930.99 | 5.779 | 27910.37805 |
| 941.31 | 8.886 | 28219.76386 |
| 957.17 | 9.116 | 28695.2347 |
| 964.13 | 0.214 | 28903.89025 |
| 972.71 | 0.519 | 29161.11218 |
| 978.42 | 0.533 | 29332.29368 |
| 986.96 | 9.955 | 29588.31643 |
| 1007.62 | 2.311 | 30207.68765 |
| 1017.83 | 6.729 | 30513.77575 |
| 1029.65 | 0.059 | 30868.13044 |
| 1041.28 | 3.848 | 31216.78907 |
| 1047.66 | 10.789 | 31408.05665 |
| 1075.43 | 7.279 | 32240.58031 |
| 1096.16 | 90.5 | 32862.05008 |
| 1100.02 | 38.732 | 32977.76996 |
| 1104.11 | 170.566 | 33100.38508 |
| 1124.34 | 48.975 | 33706.86522 |
| 1160.94 | 1.009 | 34804.10562 |
| 1173.06 | 0.653 | 35167.45408 |
| 1223.67 | 1.858 | 36684.70371 |
| 1235.77 | 250.109 | 37047.45258 |
| 1248.66 | 27.666 | 37433.88506 |
| 1252.76 | 34.813 | 37556.79997 |
| 1266.45 | 36.227 | 37967.21584 |
| 1295.06 | 55.499 | 38824.92207 |
| 1304.86 | 11.617 | 39118.71867 |
| 1308.39 | 72.373 | 39224.54541 |
| 1323.08 | 0.9 | 39664.94053 |
| 1327.07 | 1.115 | 39784.55772 |
| 1344.79 | 0.713 | 40315.78996 |
| 1348.62 | 1.393 | 40430.61047 |
| 1356.6 | 1.303 | 40669.84485 |

ISSN 2075-8545 (online)



Continuation of the table 10

| Frequency, $cm^{-1}$ | Intensity, km/mol | Frequency, GHz |
|---|---|---|
| 1366.65 | 6.555 | 40971.13627 |
| 1382.97 | 0.399 | 41460.39756 |
| 1385.78 | 14.103 | 41544.63924 |
| 1396.3 | 4.341 | 41860.02091 |
| 1408.07 | 8.986 | 42212.87663 |
| 1414.65 | 26.854 | 42410.14007 |
| 1419.76 | 8.025 | 42563.33402 |
| 1441.9 | 1.849 | 43227.07452 |
| 1472.23 | 0.511 | 44136.34504 |
| 1548.59 | 7.743 | 46425.56025 |
| 1576.03 | 12.235 | 47248.19076 |
| 1658.89 | 351.456 | 49732.27107 |
| 1674.47 | 318.638 | 50199.34771 |
| 2641.04 | 4.868 | 79176.38733 |
| 2641.32 | 52.917 | 79184.78152 |
| 2652.92 | 31.788 | 79532.54077 |
| 2665.56 | 33.243 | 79911.47843 |
| 2687.34 | 18.641 | 80564.42641 |
| 2705.95 | 14.62 | 81122.34017 |
| 2712.14 | 103.301 | 81307.9117 |
| 2715.66 | 11.926 | 81413.43865 |
| 2721.45 | 23.145 | 81587.01848 |
| 2765.65 | 5.958 | 82912.10115 |
| 2893.39 | 42.332 | 86741.65001 |
| 2946.02 | 37.782 | 88319.45771 |
| 2979.68 | 3.343 | 89328.55913 |
| 3001.52 | 17.068 | 89983.30585 |
| 3447.18 | 179.288 | 103343.85654 |
| 3553 | 110.917 | 106516.26033 |

**Table 11.** Spatial coordinates of anhydride adduct

| 01 | | | |
|---|---|---|---|
| **Atom** | **x** | **y** | **z** |
| C | 1.3141048 | –0.8258545 | 0.7555059 |
| C | 1.8636569 | 0.5797013 | 1.1233108 |
| C | 1.3136704 | –0.8260783 | –0.7556297 |
| C | 0.9459339 | 1.6700943 | 0.6886091 |
| C | 0.9453752 | 1.6699677 | –0.6888182 |
| C | 1.8627855 | 0.5794921 | –1.1241021 |
| C | 2.9091976 | 0.7381951 | –0.0008188 |
| C | –0.0067794 | –1.5607134 | 1.1291011 |
| C | –0.0072583 | –1.5613396 | –1.1282846 |
| C | 0.0056923 | –2.6205850 | 0.0007008 |
| C | –1.3502770 | –0.8831259 | –0.7584379 |
| C | –1.3499481 | –0.8826069 | 0.7593555 |
| C | –1.6585750 | 0.5329433 | –1.0952327 |
| C | –1.6581462 | 0.5337199 | 1.0952492 |
| O | –1.8547783 | 1.2974647 | –0.0002341 |

ISSN 2075-8545 (online)



Continuation of the table 11

| 01 | | | |
|---|---|---|---|
| **Atom** | **x** | **y** | **z** |
| O | –1.7655017 | 0.9622375 | –2.2325926 |
| O | –1.7646851 | 0.9638282 | 2.2323242 |
| H | 2.1217957 | –1.5260150 | 1.0874806 |
| H | 2.1868443 | 0.6667752 | 2.1819437 |
| H | 2.1212860 | –1.5262038 | –1.0878534 |
| H | 0.4548516 | 2.4031158 | 1.3144979 |
| H | 0.4537700 | 2.4029058 | –1.3143913 |
| H | 2.1851463 | 0.6664242 | –2.1829953 |
| H | 3.7010840 | –0.0469545 | –0.0010657 |
| H | 3.4147047 | 1.7347850 | –0.0011056 |
| H | 0.0020068 | –1.9061375 | 2.1848889 |
| H | 0.0011191 | –1.9073439 | –2.1838870 |
| H | –0.8832067 | –3.2961578 | 0.0010851 |
| H | 0.9121854 | –3.2713050 | 0.0006845 |
| H | –2.1844541 | –1.5229043 | –1.1293408 |
| H | –2.1840079 | –1.5220869 | 1.1310275 |

**Table 12.** Calculated FT-IR spectroscopy values for anhydride adduct

| Frequency, $cm^{-1}$ | Intensity, km/mol | Frequency, GHz |
|---|---|---|
| 410.34 | 20.798 | 12301.68372 |
| 447.04 | 0.108 | 13401.92204 |
| 452.81 | 0.34 | 13574.90229 |
| 512.65 | 0.083 | 15368.86036 |
| 540.11 | 2.66 | 16192.09045 |
| 583.31 | 11.284 | 17487.19387 |
| 603.5 | 2.094 | 18092.47484 |
| 623.11 | 7.605 | 18680.36785 |
| 634.16 | 5.53 | 19011.63852 |
| 649.2 | 2.209 | 19462.52637 |
| 704.06 | 0.195 | 21107.1878 |
| 722.3 | 8.026 | 21654.00924 |
| 743.4 | 7.966 | 22286.57133 |
| 803.65 | 6.472 | 24092.82089 |
| 812.01 | 71.561 | 24343.44738 |
| 822.12 | 5.752 | 24646.53756 |
| 836.74 | 4.914 | 25084.83413 |
| 850.63 | 1.196 | 25501.24585 |
| 866.8 | 23.662 | 25986.01026 |
| 888.17 | 0.285 | 26626.66674 |
| 900.77 | 27.931 | 27004.40524 |
| 924.88 | 3.645 | 27727.20486 |
| 930.61 | 7.682 | 27898.98593 |
| 943.97 | 0.001 | 28299.50866 |
| 977.26 | 3.81 | 29297.51775 |
| 978.09 | 0.077 | 29322.40052 |
| 1001.16 | 3.327 | 30014.02173 |
| 1006.85 | 4.062 | 30184.60363 |

ISSN 2075-8545 (online)



Continuation of the table 12

| Frequency, $cm^{-1}$ | Intensity, km/mol | Frequency, GHz |
|---|---|---|
| 1030.99 | 35.867 | 30908.30263 |
| 1050.49 | 1.817 | 31492.89792 |
| 1059.63 | 8.584 | 31766.90823 |
| 1060.77 | 1.805 | 31801.08457 |
| 1082.62 | 7.888 | 32456.13109 |
| 1086.62 | 2.614 | 32576.04807 |
| 1116.28 | 0.009 | 33465.2325 |
| 1140.17 | 9.58 | 34181.43668 |
| 1190.55 | 2.941 | 35691.79109 |
| 1190.79 | 5.585 | 35698.98611 |
| 1207.73 | 11.332 | 36206.83453 |
| 1221.86 | 170.62 | 36630.44127 |
| 1232.36 | 30.557 | 36945.22335 |
| 1247.26 | 0.763 | 37391.91412 |
| 1252.95 | 0.017 | 37562.49603 |
| 1277.51 | 6.069 | 38298.7863 |
| 1297.27 | 26.617 | 38891.1762 |
| 1304.24 | 160.98 | 39100.13154 |
| 1319.25 | 2.267 | 39550.12002 |
| 1323.33 | 9.511 | 39672.43534 |
| 1348.88 | 0.154 | 40438.40507 |
| 1353.42 | 0.543 | 40574.51085 |
| 1358.26 | 4.683 | 40719.6104 |
| 1359.97 | 6.721 | 40770.87491 |
| 1376.71 | 0.099 | 41272.72749 |
| 1378.17 | 0.068 | 41316.49718 |
| 1388.08 | 20.313 | 41613.59151 |
| 1399.99 | 16.719 | 41970.64433 |
| 1410 | 14.426 | 42270.73658 |
| 1428.49 | 0.831 | 42825.05283 |
| 1449 | 3.392 | 43439.92716 |
| 1450.76 | 3.7 | 43492.69064 |
| 1490.06 | 0.136 | 44670.875 |
| 1538.8 | 3.651 | 46132.06344 |
| 1542.11 | 9.08 | 46231.29474 |
| 1659.2 | 538.551 | 49741.56463 |
| 1757.81 | 122.141 | 52697.81806 |
| 2585.12 | 16.98 | 77499.9479 |
| 2612.64 | 32.105 | 78324.97675 |
| 2650.31 | 62.449 | 79454.29494 |
| 2655.43 | 38.88 | 79607.78867 |
| 2659.4 | 3.407 | 79726.80628 |
| 2674.23 | 46.842 | 80171.3985 |
| 2676.19 | 3.902 | 80230.15782 |
| 2683.17 | 53.369 | 80439.41295 |
| 2711.71 | 1.28 | 81295.02063 |
| 2714.1 | 120.37 | 81366.67103 |
| 2717.61 | 29.596 | 81471.89818 |
| 2721.58 | 24.989 | 81590.91578 |
| 2986.73 | 0.033 | 89539.91281 |
| 3006.64 | 2.433 | 90136.79959 |

ISSN 2075-8545 (online)



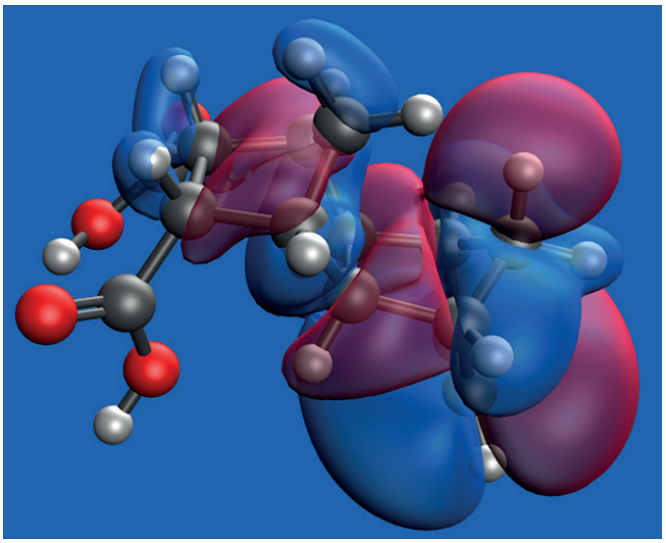

**Fig. 14.** Model of an acid-type adduct molecule with isolated molecular orbitals

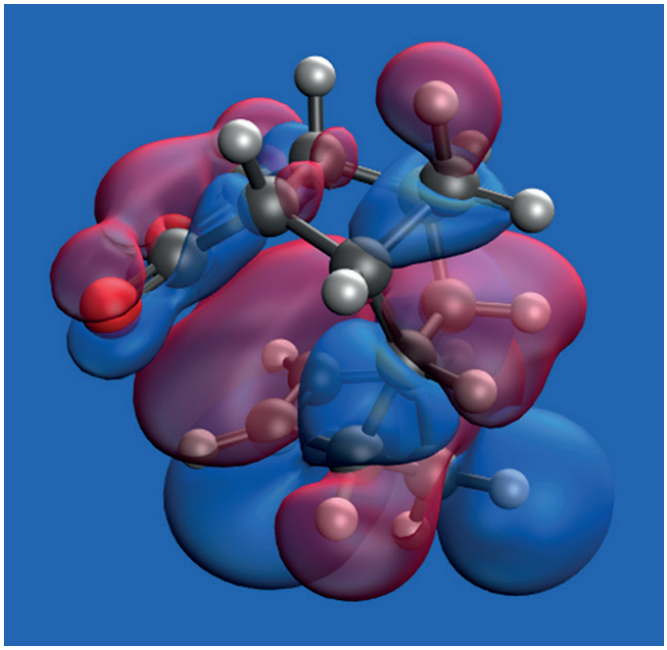

**Fig. 15.** Model of an anhydride adduct molecule with isolated molecular orbitals

the tensile strength and compression strength of the final epoxy structures due to the twisting of polymer chains. The possibility of obtaining other conformations of the compounds is also explored.

One of the major performance properties of the material is resistance to high temperatures. As follows from the data of Fig. 16, MA has low temperature resistance and is subject to structural transformations. Noticeable destruction begins at 100–110 °C. The study was conducted on a solid crystal of maleic anhydride (MA), indicating that the rate of degradation increases as the particle size decreases.

The results of the TGM adduct (Fig. 17), on the contrary, demonstrate an increase in resistance to temperatures relative to DCPD (evaporates at 40–60 °C, does not reach the operating temperature of the measuring equipment) and MA, destruction begins at 150 °C. Noticeable structural changes also begin to occur at 140–150 °C, which meets the requirements for polymer composites for space applications.

Differentiation of TGM indicators (DTGM) (Fig. 18) shows a smoother change in the course of adduct destruction relative to maleic anhydride, which, from an

ISSN 2075-8545 (online)



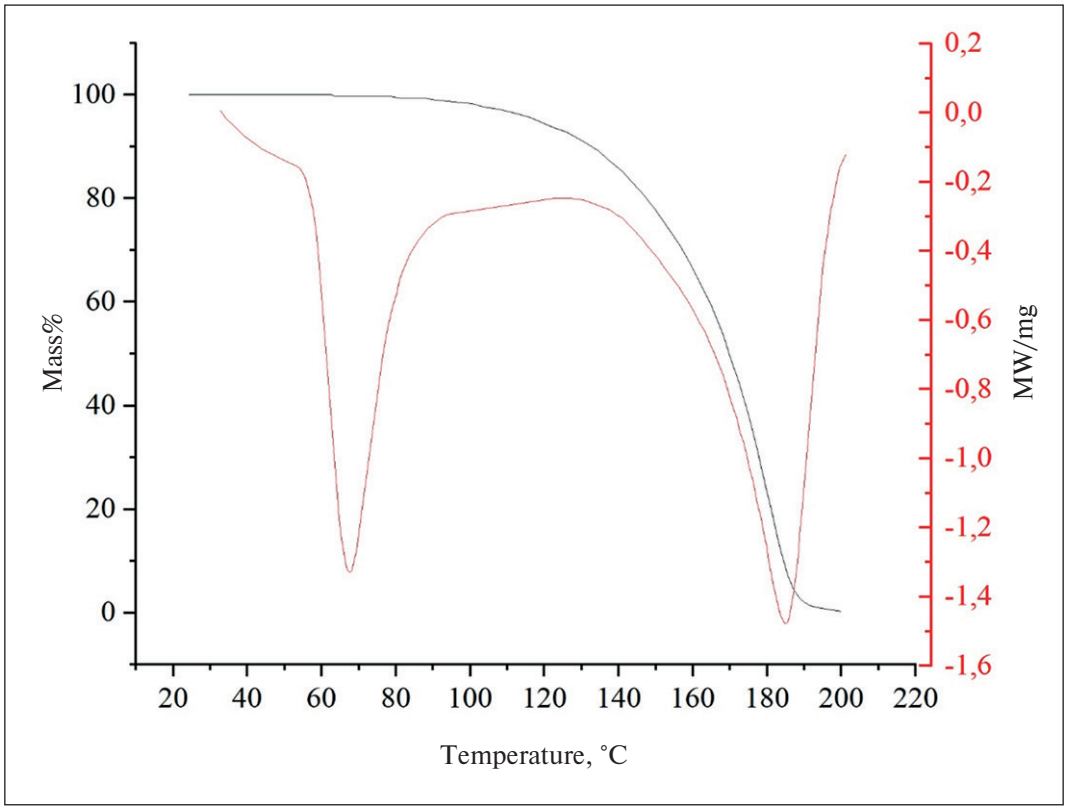


**Fig. 16.** Thermogravimetric Analysis of Maleic Anhydride

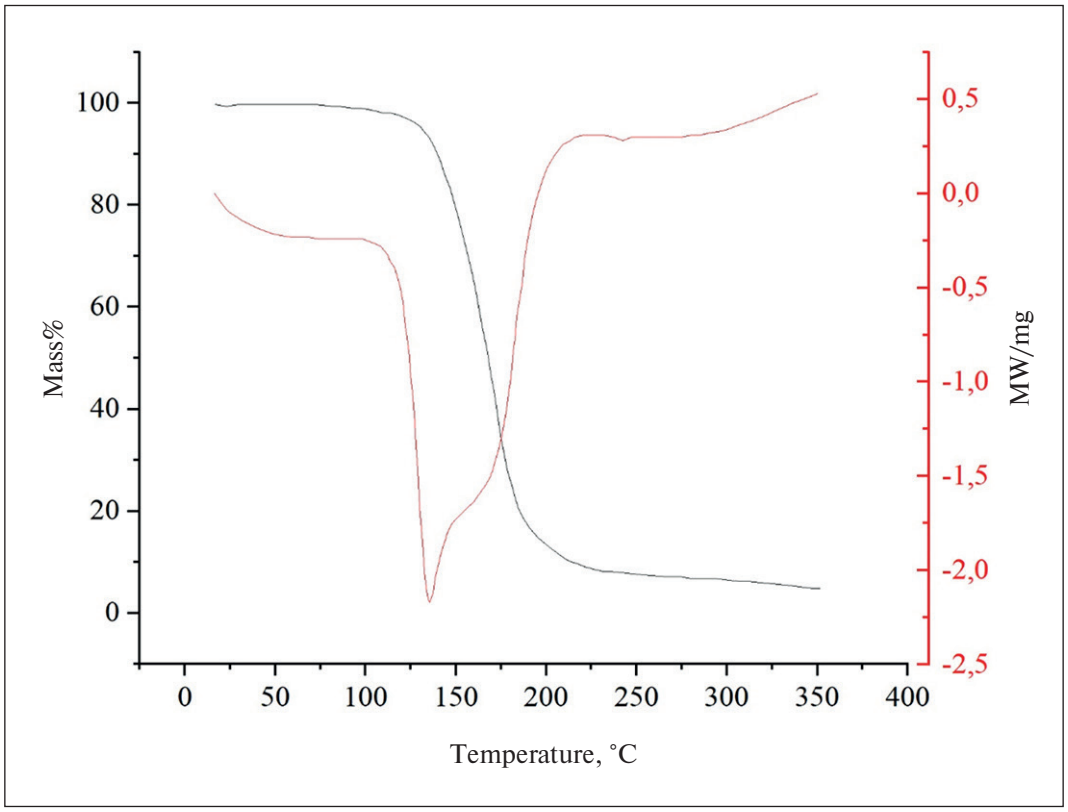


**Fig. 17.** Thermogravimetric Adduct Analysis

ISSN 2075-8545 (online)



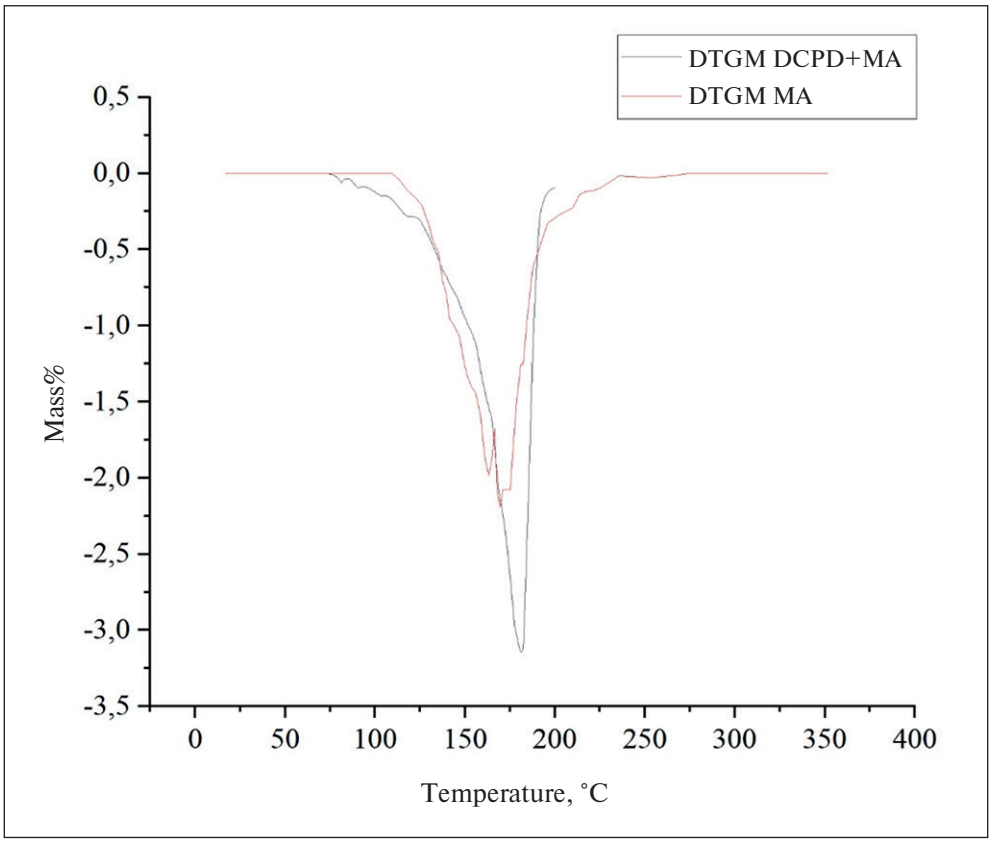


**Fig. 18.** DTGM adduct and MA curves

engineering point of view, facilitates the subsequent prediction of the mechanical parameters of the composite when calculating loads on composites.

## CONCLUSION

The use of two-component functional epoxy resins is the most promising approach for producing self-healing materials. Their broad, tunable temperature range and branched structure, combined with high reactivity, yield a more reliable final material from an engineering standpoint compared to other composite systems.

As a result of the research, a heat-resistant (up to 150 °C) epoxy resin hardener has been obtained, which is confirmed by the results of thermogravimetric analysis. Calculations performed using density functional theory (DFT) confirmed the formation of adducts from the reaction between DCPD and MA. The resulting adduct is suitable for use as a hardener for epoxy resins in self-healing polymer composites.

## REFERENCES

1. Kanu N.J., Gupta E., Vates U.K., Singh G.K. Self-healing composites: A state-of-the-art review. *Composite Part A*. 2019; 121:474–486. https://doi.org/10.1016/j.compositesa.2019.04.012. – EDN: VWZXCK

2. Priyadarsini M., Sahoo D.R., Biswal T. A new generation self-healing composite materials. *Materials Today: Proceedings*. 2021; 47:1229–1233. https://doi.org/10.1016/j.matpr.2021.06.456. – EDN: YNPYCU

3. Das R., Melchior C., Karumbaiah K.M. Self-healing composites for aerospace applications. *Advanced composite materials for aerospace engineering*. 2016; 333–364. https://doi.org/10.1016/B978-0-08-100037-3.00011-0

4. Kontiza A., Kartsonakis I.A. Smart composite materials with self-healing properties: A review on design and applications. *Polymers*. 2024; 16(15):2115. https://doi.org/10.3390/polym16152115. – EDN: COXYEL

5. Hia I.L., Vahedi V., Pasbakhsh P. Self-healing polymer composites: prospects, challenges, and applications. *Polymer Reviews*. 2016; 56(2):225–261. https://doi.org/10.1080/15583724.2015.1106555

ISSN 2075-8545 (online)



6. Mobaraki M., Ghaffari M., Mozafari M. Basics of self-healing composite materials. *Self-healing composite materials*. 2020; 15–31. https://doi.org/10.1016/B978-0-12-817354-1.00002-8

7. Islam S., Bhat G. Progress and challenges in self-healing composite materials. *Materials advances*. 2021; 2(6):1896–1926. https://doi.org/10.1039/D0MA00873G. – EDN: QHNMAC

8. Wang Y., Pham D.T., Ji C. Self-healing composites: A review. *Cogent Engineering*. 2015; 2(1): 1075686. https://doi.org/10.1080/23311916.2015.1075686. – EDN: XUODAT

9. Adil M. M., Rabbi M. S., Tasnim T. Development of microcapsule-based self-healing composite: A critical review on influencing factors of microencapsulation, healing efficiency, thermal stability and application. *Alexandria Engineering Journal*. 2025; 122:1–17. https://doi.org/10.1016/j.aej.2025.02.092. – EDN: CSNNAR

10. Ramezani M.J., Rahmani O., Ebrahimnezhad-Khaljiri H. Effect of graphene nanoplates in self-healing composite containing urea-formaldehyde microcapsules under tensile and interlaminar shear strength tests. *Results in Engineering*. 2025;106357. https://doi.org/10.1016/j.rineng.2025.106357. – EDN: KMQDRG

11. Paladugu S.R.M., Sreekanth P.S.R., Sahu S.K., Naresh K., Karthick S.A., Venkateshwaran N., Ramoni M., Mensah R.A., Das O., Shanmugam R. A comprehensive review of self-healing polymer, metal, and ceramic matrix composites and their modeling aspects for aerospace applications. Materials. 2022; 15(23):8521. https://doi.org/10.3390/ma15238521. – EDN: QFSGNS

12. Kumar E.K., Patel S.S., Kumar V., Panda S.K., Mahmoud S.R., Balubaid M. State of art review on applications and mechanism of self-healing materials and structure. *Archives of Computational Methods in Engineering*. 2023; 30(2):1041–1055. https://doi.org/10.1007/s11831-022-09827-3. – EDN: XCARXF

13. Yao Jialan, Yang Chenpeng, Zhu Chengfei, Hou Baoqing. Preparation Process of Epoxy Resin Microcapsules for Self - healing Coatings. *Progress in Organic Coatings*. 2019; 132:440–444. https://doi.org/10.1016/j.porgcoat.2019.04.015

14. Wenjing Jiang, Gang Zhou, Cunmin Wang, Yifang Xue, Chenxi Niu. Synthesis and self-healing properties of composite microcapsule based on sodium alginate/melamine-phenol–formaldehyde resin. *Construction and Building Materials*. 2021;271:121541. https://doi.org/10.1016/j.conbuildmat.2020.121541

15. Irzhak V.I., Uflyand I.E., Dzhardimalieva G.I. Self-healing of polymers and polymer composites. *Polymers*. 2022; 14(24):5404. https://doi.org/10.3390/polym14245404. – EDN: XOKPYG

16. Shebaz J.P.A., Meenakshisundaram O., Subramanian P.G. Review of self-healing strategies contributing to sustainable resilience in polymer composite systems. *International Journal of Polymer Analysis and Characterization*. 2026; 1–26. https://doi.org/10.1080/1023666X.2025.2611052

17. Xiuxiu Liu, Hairui Zhang, Jixiao Wang, Zhi Wang, Shichang Wang. Preparation of epoxy microcapsule based self-healing coatings and their behavior. *Surface and Coatings Technology*. 2012; 206(23):4976–4980. https://doi.org/10.1016/j.surfcoat.2012.05.133

18. Bekas D.G., Tsirka K., Baltzis D., Paipetis A.S. Self-healing materials: A review of advances in materials, evaluation, characterization and monitoring techniques. *Composites Part B: Engineering*. 2016; 87:92–119. https://doi.org/10.1016/j.compositesb.2015.09.057

19. Navarchian A.H., Najafipoor N., Ahangaran F. Surface-modified poly(methyl methacrylate) microcapsules containing linseed oil for application in self-healing epoxy-based coatings. *Progress in Organic Coatings*. 2019; 132:288–297. https://doi.org/10.1016/j.porgcoat.2019.03.029

20. Fei Yu, Hengyu Feng, Linghan Xiao, Yu Liu. Fabrication of graphene oxide microcapsules based on Pickering emulsions for self-healing water-borne epoxy resin coatings. *Progress in Organic Coatings*. 2021;155:106221. https://doi.org/10.1016/j.porgcoat.2021.106221

21. K. C. Nicolaou Prof. Dr., Scott A. Snyder, Tamsyn Montagnon Dr., Georgios Vassilikogiannakis Dr. The Diels–Alder Reaction in Total Synthesis. *Angewanted Chemie*. 2002; 41(10):1668–1698. https://doi.org/10.1002/1521-3773(20020517)41:10<1668::aid-anie1668>3.0.co; 2-z

22. Huertas D., Florscher M., Dragojlovic V. Solvent-free Diels–Alder reactions of in situ generated cyclopentadiene. *Green Chem*. 2009; 11:91–95. https://doi.org/10.1039/b813485e

23. Tianhui Liu, Yuzeng Zhao, Yining Deng, Honghua Ge, Preparation of fully epoxy resin microcapsules and their application in self-healing epoxy anti-corrosion coatings. *Progress in Organic Coatings*. 2024;188:108247. https://doi.org/10.1016/j.porgcoat.2024.108247

24. Blaiszik B.J., Sottos N.R., White S.R. Nanocapsules for self-healing materials. *Composites Science and Technology*. 2008; 68(3–4):978–986. https://doi.org/10.1016/j.compscitech.2007.07.021. – EDN: KJOSXF

25. Cherkashina N.I., Pavlenko V.I., Ruchiy A.Yu., Serebryakov S.V., Barinov R.A. Synthesis of self-healing microcapsules based on dicyclopentadiene. *Nanotechnology in Construction*. 2025; 17(2):189–200. https://doi.org/10.15828/2075-8545-2025-17-2-189-200 EDN: XIVHFT

ISSN 2075-8545 (online)



26. Tarasevich B.N. *IR spectra of the main classes of organic compounds. Reference materials.* Moscow: Lomonosov Moscow State University. 2012;54.

ADDITIONAL INFORMATION

The authors state that generative artificial intelligence technologies and technologies based on artificial intelligence were not used in the preparation of the article.

INFORMATION ABOUT THE AUTHORS

**Natalya I. Cherkashina** – Dr. Sci. (Eng.), Associate Professor, Leading Researcher, Head of the Research Laboratory "Development of Scientific and Technical Foundations for the Creation of Polymer Systems from Renewable Plant Raw Materials", UNIR, Belgorod State Technological University named after V.G. Shukhov, 308012, Belgorod, Kostyukova str., 46, Russian Federation, natalipv13@mail.ru, https://orcid.org/0000-0003-0161-3266

**Vyacheslav I. Pavlenko** – Dr. Sci (Eng.), Professor, Honorary Inventor of the Russian Federation, Head of the Department of Theoretical and Applied Chemistry, Belgorod State Technological University named after V.G. Shukhov, 308012, Belgorod, Kostyukova str., 46, Russian Federation, pavlenko.v.i@mail.ru, https://orcid.org/0000-0002-3464-1880

**Sergey V. Serebryakov** – Assistant Professor, Department of Theoretical and Applied Chemistry, Junior Researcher, Research Laboratory "Development of Scientific and Technical Foundations for the Creation of Polymer Systems from Renewable Plant Raw Materials", 308012, Belgorod State Technological University named after V.G. Shukhov, Belgorod, 46 Kostyukova St., serebr43@yandex.ru, https://orcid.org/0009-0008-0284-6647

**Artem Yu. Ruchiy** – Research Engineer of the Research Laboratory "Development of Scientific and Technical Foundations for the Creation of Polymer Systems from Renewable Plant Raw Materials", Belgorod State Technological University named after V.G. Shukhov, 308012, Belgorod, Kostyukova str., 46, Russian Federation, artiem.ruchii.99@mail.ru, https://orcid.org/0009-0000-2617-5624

**Yulia M. Samoylova** – Cand. Sci. (Eng.), Senior Lecturer of the Department of Information and Computer Technologies in the Activities of Internal Affairs Bodies, Belgorod Law Institute of the Ministry of Internal Affairs of the Russian Federation named after I.D. Putilin, 308024, Belgorod, Gorky str., 71, Russian Federation, y.samoylova.bel@mail.ru, https://orcid.org/0009-0003-8750-805X

CONTRIBUTION OF THE AUTHORS

**N.I. Cherkashina** – scientific guidance; setting the goals and objectives of the study; analysis of the research results; revision of the text of the article.

**V.I. Pavlenko** – development of research methodology; analysis of research results; conclusions of the article.

**S.V. Serebryakov** – conducting the experimental part of the study; graphical and tabular presentation of the results; writing the initial text of the article.

**A.Y. Ruchiy** – conducting the experimental part of the study; analyzing the results of the research.

**Yu.I. Samoylova** – conducting a literature review; conducting the experimental part of the study.

**The authors declare no conflict of interest.**

The article was submitted 21.02.2026; approved after reviewing 28.03.2026; accepted for publication 03.04.2026.